Journal of Engineering Issues and Solutions

Improved Soil Behavior: A Case Study of Reconstituted Soil from Khasibazar, Kathmandu

Bhim Kumar Dahal[1], Purnima Baidya[2*], Diwash Dahal[3], Diwakar KC[4,5]

[1]Department of Civil Engineering, Institute of Engineering, Pulchowk Campus, Kathmandu, Nepal
[2] Central Department of Microbiology, Kathmandu, Nepal
[3]Department of Civil Engineering, Southern Illinois University, Edwardsville, IL 62026, US
[4] Department of Civil and Environmental Engineering, University of Toledo, Ohio, USA
[5]Geotechnology LLC, 1780 Carillon Blvd, Cincinnati, OH 45240
** Corresponding author: purnima.baidya@cdmi.tu.edu.np*
Received: May 5, 2025; Revised: July 5, 2025; Accepted: July 12, 2025

https://doi.org/10.3126/joeis.v4i1.81563

Abstract

The study explores the behavior of high-plastic organic soil modified with varying cement contents (5%, 10%, and 15%) subjected to comprehensive laboratory testing. Analyses encompass physical, chemical, microstructural, and mechanical behavior assessments. The result implies that reconstitution significantly impacts physical attributes. Specific gravity initially decreases but reverts to its initial value at 15% cement content. Liquid and plastic limits increase with increasing cement content, while the plasticity index decreases initially and increases after a certain cement content. Similarly, soil minerals primarily comprising quartz, kaolinite, and biotite affect soil particle cementation and aggregation, leading to larger particle sizes, which was verified by SEM imaging, which revealed a more flocculated microstructure and larger particle sizes in cement-treated soil. Furthermore, two power functions are developed first to relate the soil strength with cement content, ranging from 89.83-601.76 kPa at 5% and 15% cement content, respectively, and second to relate failure strain with cement content, which demonstrates the enhanced brittleness characteristics of cement-treated soil. Similarly, an exponential function of cement content well represented the primary yielding strength (p'_{yi}; 10-325 kPa) when cement increased in similar percentages as above. Additionally, the UCS and p'_{yi}, are strongly correlated, following a power function. Finally, this comprehensive analysis underscores the pivotal role of cement content in soil reconstitution. It emphasizes the significant changes in its physical, chemical, microstructural, and mechanical properties, offering insights vital for mitigating challenges in infrastructure development involving lacustrine deposits.

Keywords: *Cement, Clayey soil, Lacustrine deposit, Mineralogy, Modified soil*

1. Introduction

Weak or soft soils are cohesive, fine-grained soils with high compressibility and low shear strength. Silt, clay, and organic soils are the most common types of soft soils. Low-lying areas close to bodies of water, such as rivers, lakes, and seas, are commonly habitat to several types of soil (Guo et al., 2023). Their unfavorable characteristics present considerable hurdles when constructing foundations for substantial infrastructures, potentially leading to excessive settlements or instability. Consequently, employing diverse soil improvement techniques, such as mixing, compaction, reinforcement, chemical stabilization, etc., becomes imperative to augment the resilience and stability of the structure throughout the design life (Balasubramaniam et al., 1998; Broms & Anttikoski, 1984; Jefferson et al., 2015). Previously, research has been conducted on chemical stabilization methods, including cement, lime, fly ash, rice husk ash, and their combinations (Behak, 2017; Broms, 1990; Ghosh & Subbarao, 2006; Prusinski & Bhattacharja, 1999). Some studies have explored their impact on strength development in modified soils, focusing on parameters like initial and final setting times (Kang et al., 2013) as well as the microstructure and strength behavior of treated soils (Dahal & Zheng, 2024; Kang et al., 2015, 2024). Cement-based stabilization remains the most commonly used ground improvement technique, benefiting from advancements in technology (Chew et al., 2004; Dahal et al., 2019; Dai et al., 2015; Sasanian & Newson, 2014; Uddin et al., 1997; Zhao et al., 2016). This method involves soil modification through cement mixing and compaction, or reconstitution, resulting in changes to the soil's physical, chemical, and mechanical properties. These changes depend on factors such as curing time, curing pressure, and the chemical reactions involved (Chew et al., 2004; Gui et al., 2021; Porbaha et al., 2000). The key responses in cement stabilization include dehydration, ion exchange, and pozzolanic reactions, which lead to the formation of cementitious products. Initially, hydrated gel ($C_3S_2H_3$) contributes to early-stage strength development, while pozzolanic reactions between calcium ions, soil silica, and soil alumina form hydrated calcium silicates (C-S-H) and hydrated calcium aluminates (C-A-H). These products alter the soil's microstructure by rearranging soil particles and enhancing interparticle bonding (Mitchell R.J., 1970). Research has predominantly focused on the mechanical behavior and strength of cement-treated soils, with some studies exploring both microstructural and mechanical changes. The degree of these improvements is, however, affected by factors such as cement content, curing conditions, and the initial composition of the soil. These factors govern the physicochemical interactions between cement and soil minerals, which directly affect the mechanical performance of stabilized soils, as highlighted in earlier studies (Consoli et al., 2006; Porbaha et al., 2000). In spite of this, few studies have explicitly examined the physicochemical processes and how they affect the strength and microstructure of soil. According to recent research, the plasticity index falls in reconstituted marine soils as compared to their original form, but the liquid and plastic limits rise noticeably with increasing cement presence. Furthermore, if particle size expands, denser soil structures are produced (Dahal & Zheng, 2024). Similar observations have been reported in Singapore marine clay and Ballina clay (Indraratna et al., 2016; Jan & Mir, 2018; Xiao et al., 2017), where enhanced soil strength has been correlated with these microstructural changes.

The weathering of rocks inside the valley's watershed is the primary source of soil in the Kathmandu Valley. These soils are of lacustrine and fluvial origin, consisting of clayey, silty, sandy, and gravel sediments (Katel et al., 1996). Sediments with significant recharge rates from the Gorkarna and Tokha formations, i.e., coarser-sized sediments, are found on the northern side of the Kathmandu Valley. However, in the southern and central parts of the valley, the soil mainly consists of fine-grained soil like silt and clay, with occasional presence of organic material, categorized as soft clayey soils (Shrestha et al., 2023). Soft clayey soil always has high water content, high compressibility, low permeability, and low shear strength. All these challenges lead to soil failures, such as excessive settlement and failure of the substructure, leading to consequences encompassing physical, psychological, societal, and economic impacts. Hence, the initial stage for engineers

constructing infrastructure involves conducting soil investigations. This process assesses the soil's quality, establishing its mechanical, physical, and chemical behaviors (N. K. C. & Raj Dahal, 2020). Few comprehensive studies have been conducted to evaluate the clayey soil behavior in Kathmandu Valley. Meanwhile, routine assessments of soil properties like index properties, strength, and consolidation of natural soil are performed in various infrastructure projects (S. K.C. et al., 2016; Katel et al., 1996). Additionally, some studies have explored soil improvement through compaction at optimum moisture content using additives such as cement, stone dust (Phuyal & Dahal, 2021), brick dust (Paudel & Kumar, 2022), and eggshell powder (Acharya et al., 2023). However, there is a noticeable gap in studies focusing on modified soil. This is crucial in understanding soil behavior for deep cement mixing and jet grouting, especially for major infrastructure projects in clayey soils in Kathmandu Valley and other similar areas with clayey soil deposits. Therefore, this research is focused on evaluating modified soil from Khasibazar, Kathmandu using cement and considering the soil's physical, chemical, mineralogical, microstructural, and mechanical behaviors.

2. Materials and Methods

2.1 Sample preparation

The methodology adopted in this study was similar to the method employed in the previous research by Dahal and Zheng (Dahal & Zheng, 2024). The soil sample was collected from Khasibazar (K), Kathmandu Valley, and general-purpose ordinary Portland cement (OPC) was purchased from the local market. The sample was transported to Huazhong University of Science and Technology, Wuhan, China, for further analysis. The soil was air-dried at room temperature, powdered, and mixed with different cement contents, such as 5%, 10%, and 15% (coded as K-5, K-10, and K-15) at 100% water content by dry soil mass (Kang et al., 2013). The water content for modified soil is generally maintained at 1.25 times the liquid limit (LL) or more significant than natural moisture content; the soil represents the actual field condition just after grouting. The mixture was poured into moulds and cured for 28 d (25 °C). Then, the samples were tested for physical, chemical, mineralogical, microstructural, and mechanical soil behaviors.

2.2 Experimental programs

2.2.1 Physical properties

Atterberg's limits and particle size distribution (PSD) analysis were performed to study changes in physical properties and specific gravity. For specific gravity, after 28 d of curing, the modified soil samples were oven-dried, crushed, and sieved through 4.75 mm sieve to determine specific gravity using a water pycnometer (ASTM D854-14). Additionally, the soil was sieved through 425 μm sieve to determine the liquid and plastic limit (PL) using a cone penetrometer (LG-D10). Furthermore, the soil was sieved through a 75 μm sieve for PSD analysis using the Bettersize 2000 Intelligent Laser Particle Size Analyzer (Bettersize 2000E), where sodium phosphate was used as a dispersing agent.

2.2.2 Chemical and mineralogical studies

An X-ray fluorescence (XRF) analyzer was employed to assess the chemical composition of natural soil, cement, and modified soil specimens. The analysis provided data on the various oxides present, along with their respective percentages. Additionally, X-ray diffraction (XRD) measurements were conducted within a specified 2-theta angular range, chosen based on the mineral composition of the sample. Typically, for soil samples, the angular range spans from 5- 70°. However, this study analyzed the soil samples within the 0 to 70° 2-theta angle (copper Kα radiation, λ = 1.5418, 740, V = 40 kV, I = 25 mA) (Li et al., 2013). The obtained results were interpreted using Match! 2 software to identify different minerals in the samples.

2.2.3 Mechanical behavior

Unconfined compressive strength (UCS) and isotropic compression tests were carried out to examine the mechanical behavior of cement-treated soil. The soil slurry was prepared by mixing the soil with different cement contents. The soil slurry was allowed to set and cured. The samples were tested after curing for 28 d. The UCS testing followed ASTM D2166M-16 standards, employing a standard loading frame (GDSLF50) capable of applying 50 kN load at a compression rate of 1% per minute. The stress and strain were recorded automatically, and the change in area was computed for the actual stresses during the testing process. To further evaluate the compressibility, isotropic compression tests were performed using a computer-controlled triaxial stress path apparatus. These tests followed the guidelines outlined in ASTM D4767, with a constant confining stress rate of 1 kPa/min applied until an effective confining stress of 1 MPa was reached.

2.2.4 Microstructure

The solid samples cured for 28 d were used for microstructural analysis, as shown in Figure 1(a). A scanning electron microscope (SEM) was used to produce images illustrating the surface structure of the specimens. To prepare for SEM analysis, the samples were coated with gold and carbon using a sputter coater (BAL-TEC/SCD 050) (Figure 1(b)), and the resulting images were captured using the FEI Quanta 200 Environmental Scanning Electron Microscope (Figure 1(c)), also referred to as the Variable Pressure Scanning Electron Microscope (FEI Quanta 200 ESEM/VPSEM). This instrument is well-suited for the examination of dry soil samples due to its ability to adapt to varying environmental conditions, and it provides essential high-resolution imaging capabilities crucial for soil analysis and research (Zhu et al., 2016).

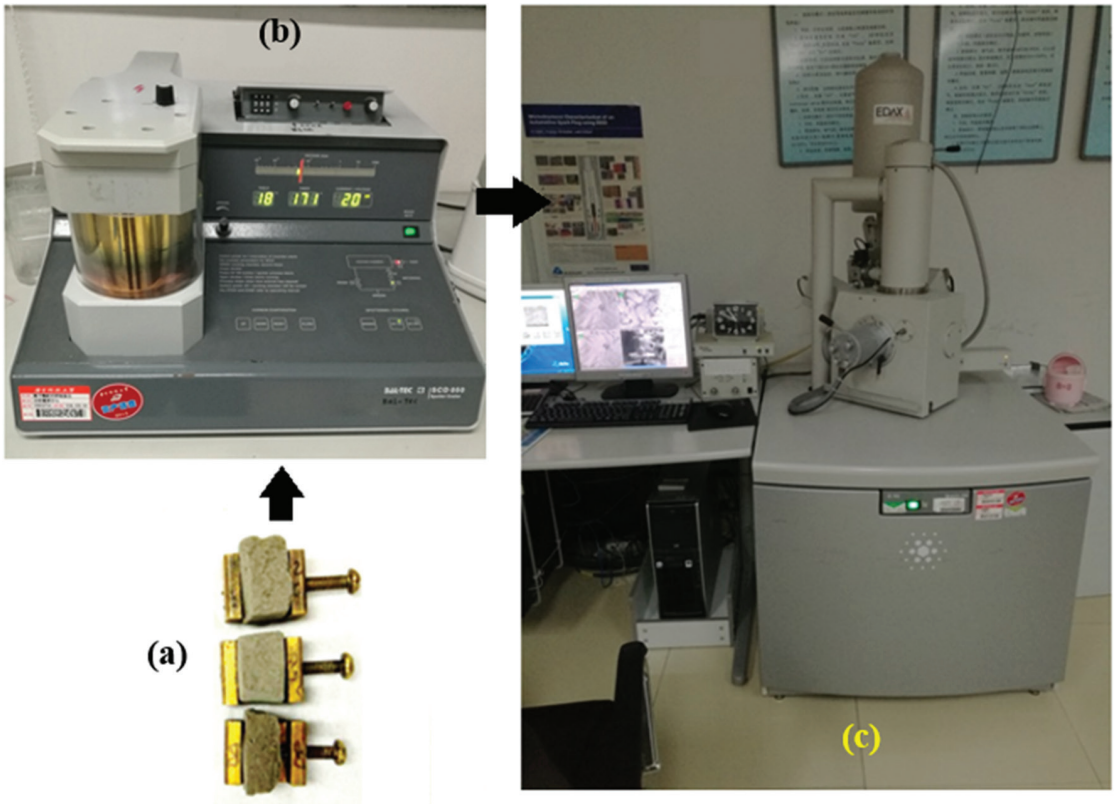

Figure 1: SEM imaging: a) Soil samples**,** b) Sputter coater BAL-TEC/SCD 050, and c) FEI Quanta 200 ESEM

3. Results and Discussion

The extensive study concentrated on the physical, chemical, and microstructural alterations in soil behavior following reconstitution with cement. An unconfined compression test was also used to evaluate the mechanical behavior. To assess the various behaviors, the soil was altered with cement contents of 5%, 10%, and 15%. The following is a discussion of the laboratory test findings.

3.1 Physical analysis

The untreated soil had LL of 62.71%, PL of 47.25%, and an organic content of 6.53% According to the unified soil classification system (USCS), the soil was High Plasticity Organic (OH).

3.2 Specific gravity

The specific gravity (Gs) of the untreated soil was 2.58. However, the Gs decreases initially as cement content increases. From the curve fitting of experimental data, approximately 8% cement content gradually increases to 2.58 on the addition of cement content to 15% (Figure 2). A study on cement-treated Bangkok clay indicated a notable decrease in Gs with higher cement content (Uddin et al., 1997). Furthermore, findings from the same research of specimens cured for 12 d align closely with the results obtained in this study. Hence, an initial increment in cement content substantially decreases the Gs of modified soil. However, beyond a certain threshold of cement content, Gs begins to increase with higher cement concentrations.

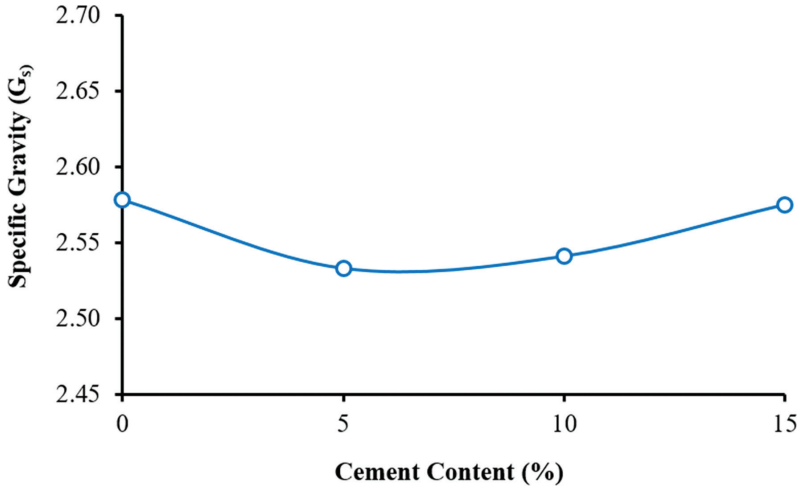

Figure 2: Specific gravity of natural and modified soils

3.3 Atterbergs' limits

The liquid limit varies with changes in cement content, as shown in Figure 3(a). The research reveals that a higher cement content leads to an increase in the LL in treated samples, similar to findings from studies on lime-treated Louiseville clay (Locat et al., 1990) and cement-treated Singapore clay. However, LL was reported to decrease slightly in Singapore clay when the cement content exceeds 10% (Chew et al., 2004). With the increase in cement content, agglomeration occurs in the soil matrix, which traps some portions of water. The water, thus trapped, does not play an active role in making the soil flowable. Although the trapped water does not play a role in the LL, it is considered during water mass calculation since free and trapped water evaporate during water content tests. Therefore, the LL increases with the addition of cement to the

soil.

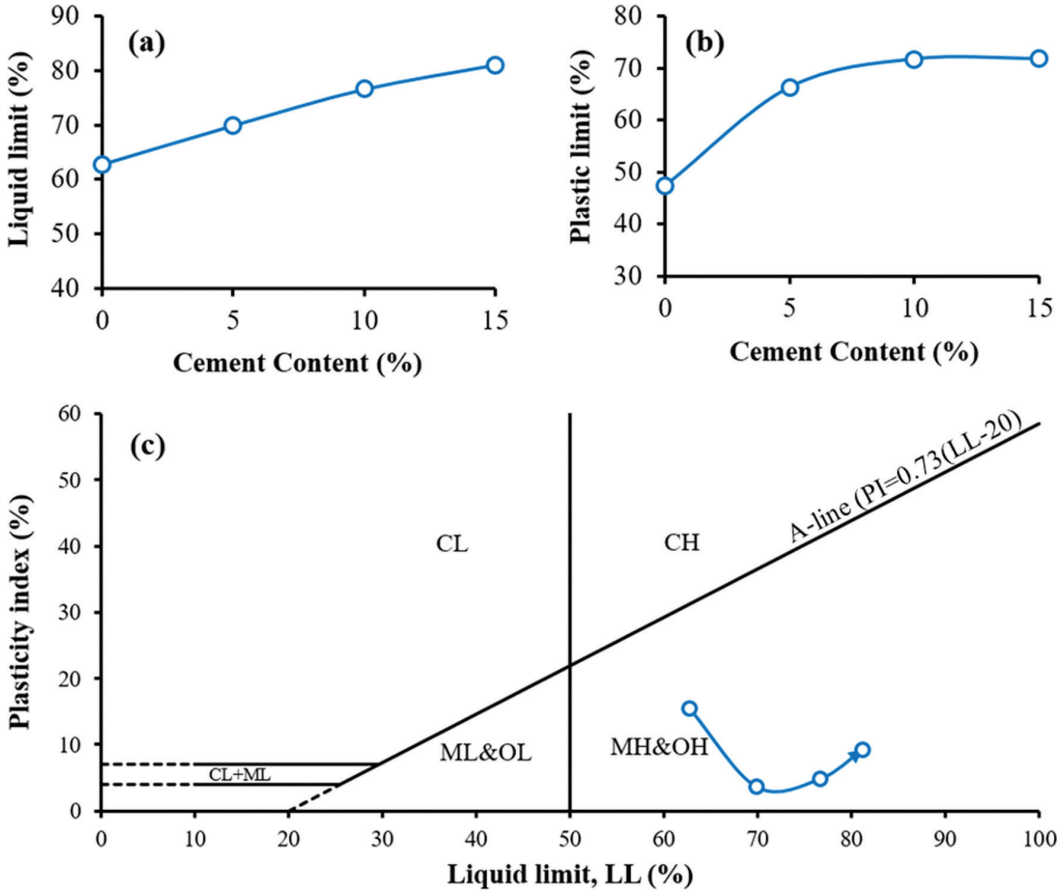

Figure 3: Soil consistency: a) Liquid limit, b) Plastic limit, and c) Plasticity index chart

The plastic limit (PL) of the modified soil samples was higher than that of untreated soil, as shown in Figure 3(b). It can be observed in the result that an increase in PL is 19.05% at 5% cement content, beyond which further increases in cement content do not significantly affect PL. A similar trend was observed in Bangkok clay (Uddin et al., 1997). The findings reveal that the LL and PL of the cement-treated soils rise as the cement content increases. However, the rate at which PL increases surpasses LL at lower cement levels, causing a sudden drop in the plasticity index (PI) (Figure 3(c)), unlike the behavior of soil treated with alkali-activated eggshell (Acharya et al., 2023). Despite PI increasing beyond specific cement contents (e.g., 5%), PI remains lower than untreated soil across all cement content ranges studied. The Atterberg's limits summary, shown on the plasticity chart based on the USCS (Figure 3(c)), indicates that the soil falls within the category of high plasticity silt or organic soil before and after reconstitution. At 5% cement content, the soil exhibits a more silty behavior. The soil regains some plasticity characteristics with increased cement content; however, it remains lower than the untreated soil. The apparent increase in PI after 5% cement content is because LL increases with cement content as water entrapped increases with agglomeration, but the PL remains nearly constant. Moreover, cement, when mixed with water, produces calcium silicate hydrates and calcium hydroxide, which enhance soil water retention capacity and LL. Similarly, cement reduces the activity of clay minerals by exchanging cations with them, thereby decreasing water adsorption. This process reduces plasticity and renders finer particles less reactive, resulting in an increased PL (Méducin et al., 2007).

3.4 Gradation analysis

The particle size distributions of both untreated and treated soil are illustrated in Figure 4. The data depict a noticeable shift in the PSD curve towards coarser particles for the treated soil, where the D_{10} increases from 3.46-4.89 µm with 15% cement content. A similar trend is evident for the mean particle size (D_{50}). This phenomenon mirrors findings observed in modifying Singapore marine clay using cement (Chew et al., 2004). The shift is attributed to increased pH levels, causing bivalent calcium ions to displace monovalent ions within the minerals. Calcium ions on the soil particle surfaces lead to aggregation and form larger particle sizes (Chew et al., 2004; Kawasaki et al., 1981). The flocculation process was also observed in the SEM images of the treated specimens, indicating a measure of the effectiveness of the improvement using cement as the chemical stabilizer.

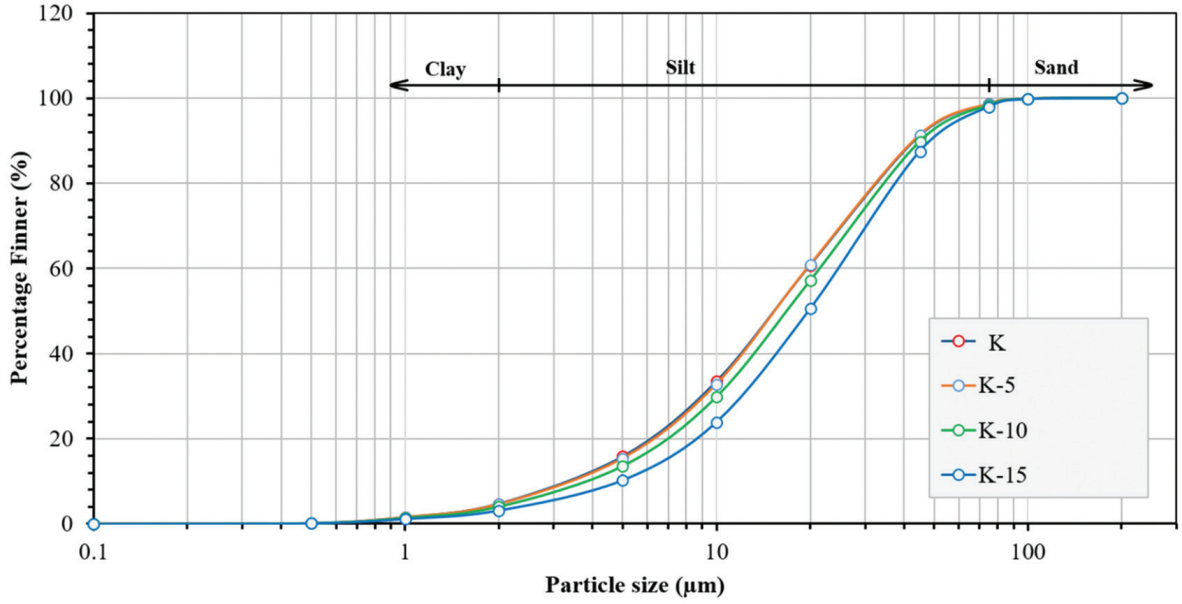

Figure 4: Variation in particle size

3.5 Chemical composition

The untreated soil has the highest Al_2O_3 content, 16.35%, which decreased by adding cement by 1.65, 6.80, and 4.34%, respectively, for K-5, K-10, and K-15 samples. The Al_2O_3 content in the cement was 6.6%, which ultimately decreased the Al_2O_3 content in the K-5, K-10, and K-15 samples. Similarly, SiO_2 content in sample K was 72.61%, reduced by 11.28, 13.19, and 12.27 percent for K-5, K-10, and K-15 samples after adding cement, as SiO_2 content in cement is 23.54%. Similarly, MnO content in K was 0.13%, which fluctuates slightly with the increase in cement content, and the changes are insignificant. However, CaO increased by 3.35, 4.16, and 4.79 folds for K-5, K-10, and K-15 samples, respectively, on the addition of cement with 57.25% CaO; therefore, the addition of cement increased the overall CaO content in all samples treated with different cement content. Similarly, Fe_2O_3 changed by 1.08, 1.12, and 0.9 folds for K-5, K-10, and K-15 samples, respectively, after adding cement, which was 3.29%. Figure 5(a), (b), and (c) show the chemical composition in different samples.

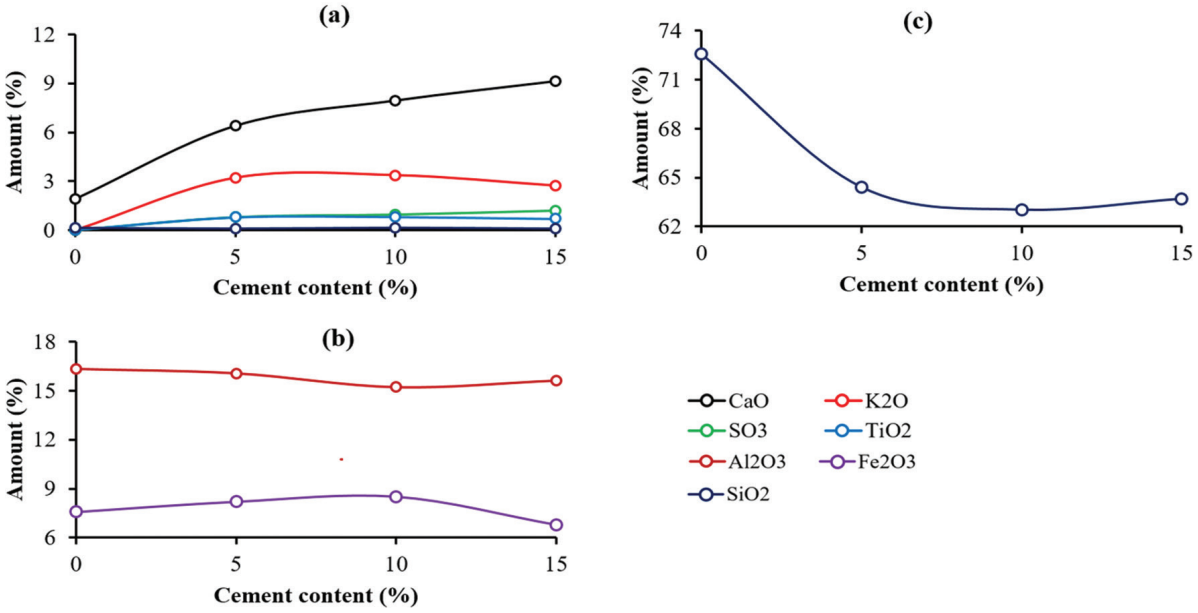

Figure 5: Chemical composition of natural and modified soils: a) Percentage of K2O, CaO, TiO2, MnO, Na2O and MgO, b) Percentage of Al2O3 and Fe2O3, and c) SiO2

3.6 Mineralogical analysis

X-ray diffraction (XRD) analysis was performed on various soil samples and admixtures using the Match! 2 program. The diffraction peaks at 2θ angles of 12.49°, 20.39°, 20.83°, 26.62°, 34.99°, 36.54°, 39.42°, 40.28°, 45.45°, 50.012°, 59.93°, 68.32°, indicate the kaolinite (Figure 5). The natural kaolinite was found at 2θ values of 12.33°, 24.82°, 26.65°, and 38.37° (Sachan & Penumadu, 2007). Similarly, diffraction peaks at 2θ angles of 20.83°, 26.62°, 36.54°, 39.43°, 40.27°, 45.45°, 50.01°, 59.93°, 68.32°, indicate the quartz (Figure 5). According to earlier research, quartz XRD peaks were around 20.85° and 26.64° for amorphous and crystal forms, respectively (Abbasi et al., 2021). Whereas diffraction peaks at 2θ angles of 8.73°, 8.84°, 8.91°, 17.77°, 17.88°, 19.92°, 20.84°, 20.81°, 20.93°, 46.54°, 39.43°, 40.27°, 44.42°, 45.45°, 59.93°, 68.32°, indicate the presence of biotite (Figure 6). Also, in a study conducted in Thailand soil, the kaolinite mineral displayed peaks at 13° and 29°, the illite mineral displayed peaks at 10° and 21°, and a peak at 31° was found for the quartz crystals (Saminpanya & Denkitkul, 2020). In addition, a diffraction peak at 19.73° was observed for montmorillonite minerals (Fil et al., 2014). The diffraction peaks at 2θ angles of 29.37°, 29.47°, 29.91°, 39.43°, indicate the presence of calcite. Moreover, the distinctive peaks of calcite at 26.5°, 27.7°, 33.4°, 45.9°, and 51.5° are seen in the XRD study (Dehghani et al., 2019).

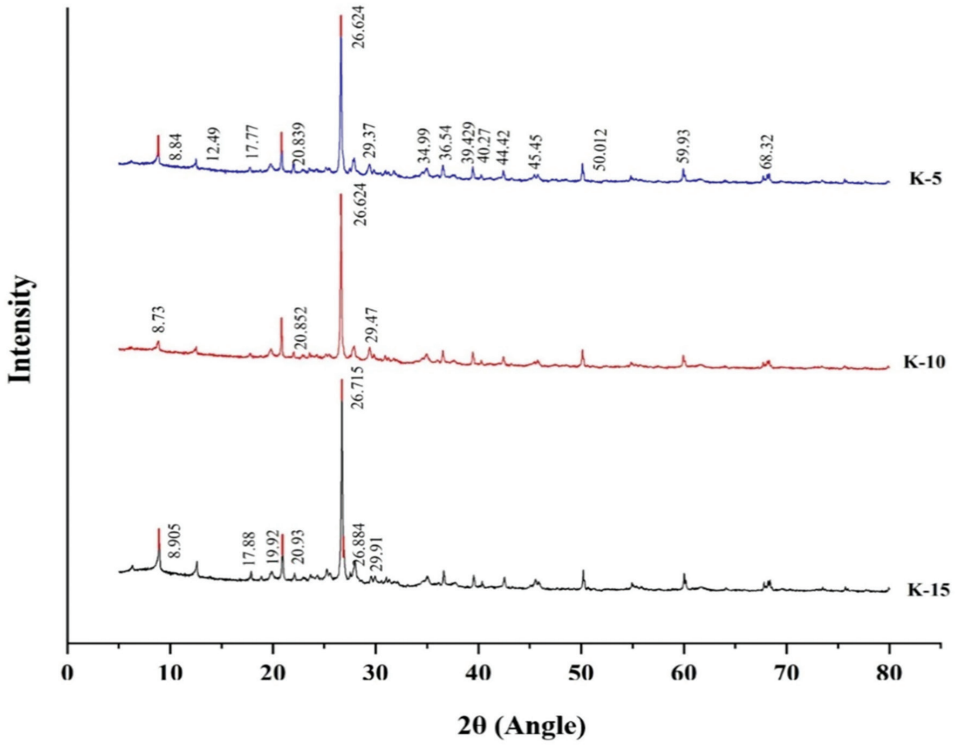

Figure 5: Variation in mineralogical composition with cement contents

3.7 Microstructural analysis

The SEM was utilized for analysis, and feature extraction was performed on specimens after 28 d of curing. The analyzed samples, K-0 and K-10, indicate notable flocculation in the soil microstructure, with average particle sizes of 6.68 μm and 16.89 μm, respectively, observed under a 5000× magnification field (Figure 7 (a.1), (a.2), (b.1) and (b.2)). In the case of K-10, a cotton liked structure of calcium silicate hydrates were observed which was identical to the SEM micrographs to those previously published (Chhabra & Ransinchung Rongmei Naga, 2023). Additionally, a mixture of flat, rhombic crystals was observed, which was shown by CaO (Garcia et al., 2022). In contrast, the fibrous structure of calcium aluminum hydrates was also observed and identical to the FESEM micrographs to those previously published literature (Qu et al., 2018). The development of the microstructure of cement-treated soil was seen as a result of the hydration and subsequent pozzolanic reactions. Although the aggregation of soil clusters forming the large soil particles was evident, some precipitated crystals were found individually or as clusters, creating the cementation bonds between the soil particles. Such observations were reported from the study of Singapore marine clay, Ballina clay, and Hanzhou dredged marine soil, where the degree of reticulation increase was prominent with an increase in cement content(Chai et al., 2018; Dahal & Zheng, 2024; Kamruzzaman et al., 2006).

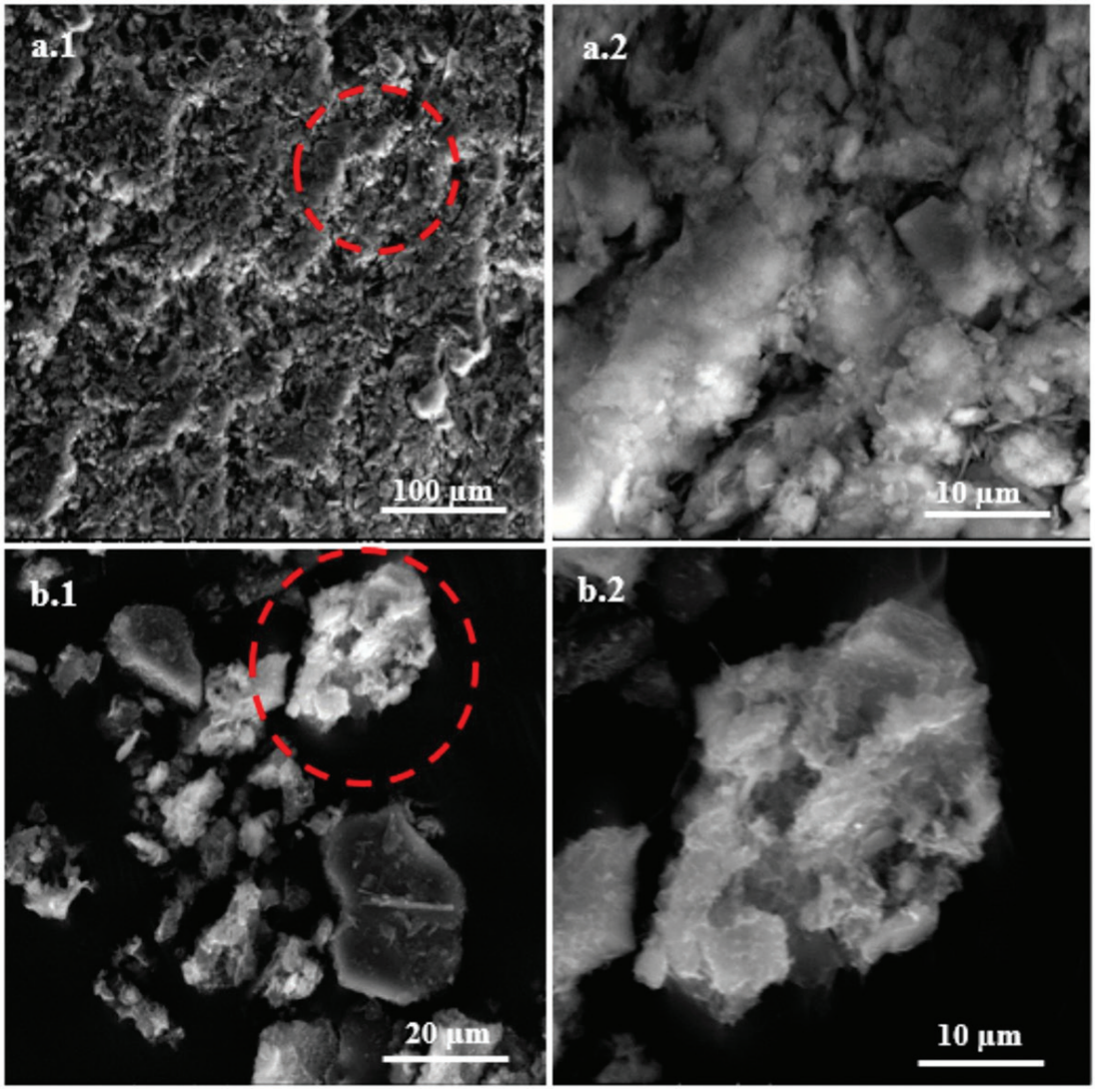

Figure 6: SEM photographs of natural and modified soils observed under 5000× magnification field

3.8 Mechanical behavior

The results of unconfined compression tests of soil representing different mechanical behavior with varying cement contents are presented in Figure 8. Figure 8(a) showed that the K-5 sample has the lowest strength among all; the mobilized strength increased with the increase in strain and reached the maximum value (q_u = 89.83 kPa) and then decreased with the further increase in strain. At 10% cement content, the peak value (q_u = 263.19 kPa) increased almost four times. Similarly, at 15% cement content, the $q_f$was 601.76 kPa. The failure stress and failure strain (ε_f) were plotted, and a power function represented a unique relation. The relation is presented in equation (1) with the goodness of fit as R^2=0.96. Similarly, a power relationship of q_u and cement content (A_w) was obtained as the best fit. The mathematical relation is given in equation (2), which has R^2=0.99. The results demonstrate that soil strength improves significantly with increased cement content (Figure 8(b)) and the trend observed is aligned with the different studies on cement-treated soils (Dahal & Zheng, 2024; Horpibulsuk et al., 2003; Miura et al., 2001; Tan et al., 2002).

$$q_u = 859.26\ \varepsilon_f^{-2.226} \quad (1)$$

$$q_u = 5.446\ A_w^{1.712} \quad (2)$$

The increase in cement content decrease ε_f, resulting in the brittle behavior of cement-treated soil. The average failure strains for K-5, K-10, and K-15 were 2.82%, 1.54%, and 1.26%, respectively. A power relationship of ε_f and A_w was also developed. The mathematical relation is given in equation (3) which has the R^2=0.98 (Figure 8(c)).

$$\varepsilon_f = 9.215\ A_w^{-0.749} \quad (3)$$

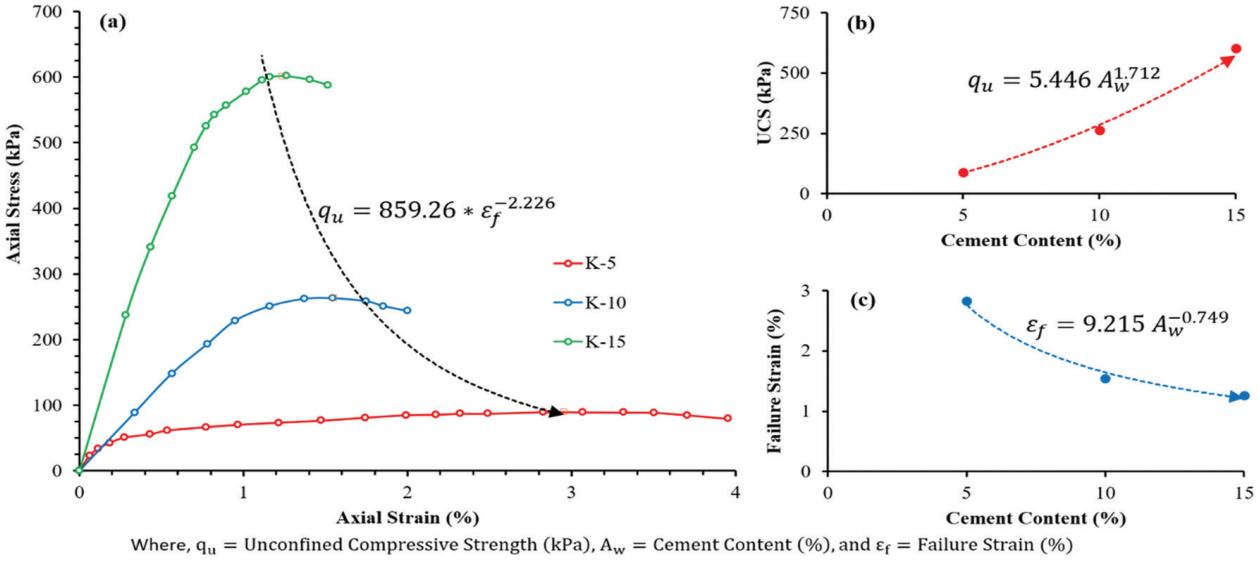

Figure 7: Mechanical behavior: a) Stress-strain behavior, b) Increased strength with cement content, and c) Increased brittleness with cement content

Similarly, isotropic compression results indicate that the primary yielding strength (p_{yi}) of the treated soil with 5% cement content was 10 kPa, which increased to 325 kPa when the cement content was raised to 15% (Figure 9(a)). This p_{yi} reflects the cementation effect, which is further confirmed by the SEM analysis showing that the cement-treated soil with higher cement content exhibits a more dispersed microstructure and larger particle size. Additionally, the cement content had little impact on the compression indices, which were found to be similar across 5%, 10%, and 15% cement contents, with λ values of 0.369, 0.379, 0.387and κ values of 0.020, 0.020, 0.021, respectively. The results of this study showed slightly higher p_{yi} and reduced compressibility compared to treated marine soil from a similar study, though it exhibited slightly more swelling during unloading (Dahal et al., 2019). Statistical analysis revealed an exponential relationship between p_{yi}, and cement content (Figure 9(b)), while a power function described the relationship between q_u and found that p_{yi} (Figure 9(c)), as indicated by equations (4) and (5). The R^2 for both equations exceeded 0.99, demonstrating a high goodness of fit and predictability

$$p'_{yi} = 1.73\ e^{0.348\ A_w} \quad (4)$$

$$q_u = 26.676\left(p'_{yi}\right)^{0.547} \quad (5)$$

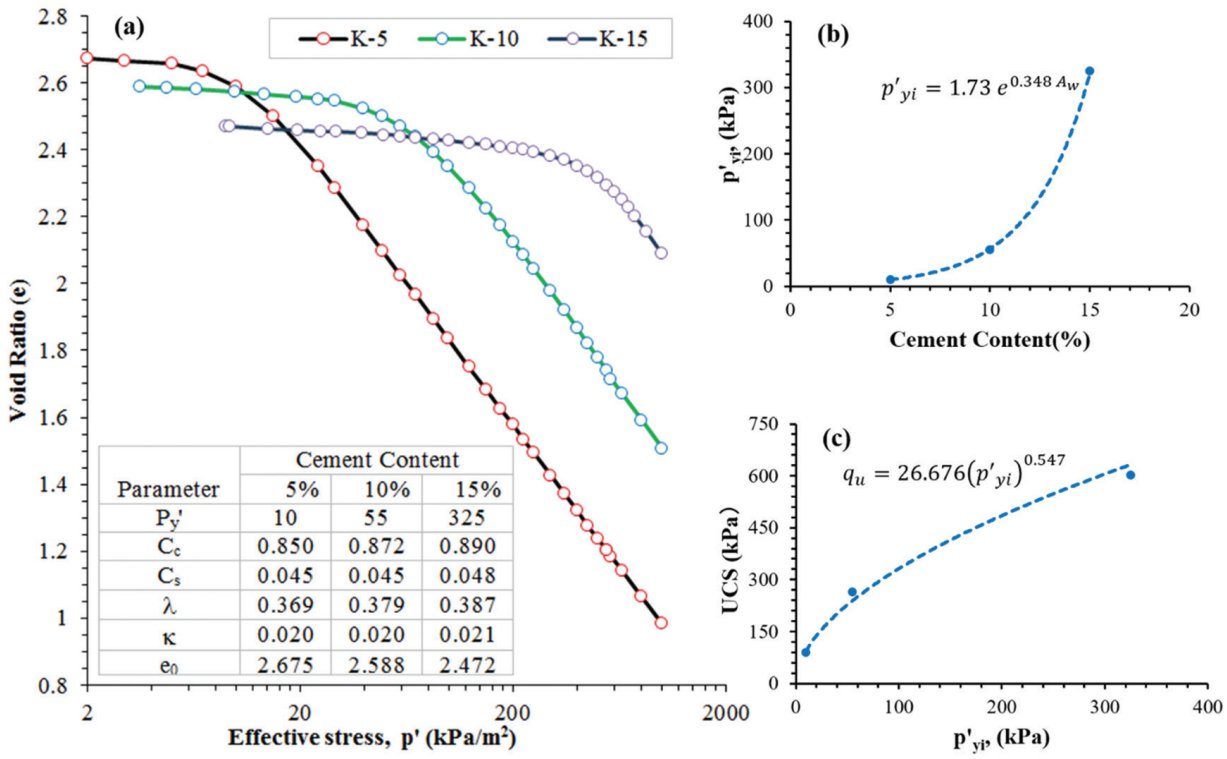

Figure 8: Mechanical behavior: a) Isotropic compression, b) Variation of primary yielding strength with cement content, and c) Relation between primary yielding strength and UCS

4. Conclusions

The soil from Khasibazar, Kathmandu is modified with different cement contents and used for laboratory tests. The results are analyzed to determine the physical, chemical, microstructural, and mechanical behavior. The findings of this study are summarized below.

- Cement content notably impacts the physical properties of treated soils, i.e., specific gravity, liquid limit, plastic limit, and plasticity index.
- The addition of OPC significantly influenced the natural soil's composition (such as Al_2O_3, SiO_2, SO_3, K_2O, CaO, TiO_2, MnO, Fe_2O_3, Na_2O, and MgO), with quartz being the primary compound found on modified soil, followed by kaolinite and biotite.
- The influence of cement content on clay particle cementation and aggregation is evident, leading to larger particle sizes. For instance, D_{10} increased from 3.458 µm to 4.889 µm with 15% cement content. SEM image analysis supports these findings, showcasing a more flocculated microstructure, larger particle sizes, and increased voids in treated soil compared to untreated soil. These microstructural changes are pivotal in augmenting the modified soil's mechanical behavior.
- The soil displays increased brittleness and strength with increasing cement content, following a power-law relationship with R^2 exceeding 0.98. The UCS increases significantly, ranging from 89.83 kPa at 5% cement content to 601.76 kPa at 15% cement content.

- The p_{yi} of the treated soil shows a significant increase as the cement content rises, ranging from 10-325 kPa when the cement proportion increases from 5-15%. This relationship follows an exponential function with an R^2 value greater than 0.99. Additionally, both the UCS and p_{yi} are strongly correlated, following a power function with an R^2 value above 0.99.

Overall, this investigation underscores the significant influence of cement content on the physical, chemical, microstructural, and mechanical characteristics of treated soil, shedding light on crucial parameters essential for enhancing soil behavior and performance. However, to generalize these findings, further studies are needed considering varying curing periods, different types or contents of cement and additives, as well as different soil types from across the Kathmandu Valley.

Acknowledgements

The Analytical and Testing Center, Huazhong University of Science and Technology, provided raw XRD, XRF, and SEM data.

References

Abbasi, F., Hashemi, H., Samaei, M. R., SavarDashtaki, A., Azhdarpoor, A., & Fallahi, M. J. (2021). The synergistic interference effect of silica nanoparticles concentration and the wavelength of ELISA on the colorimetric assay of cell toxicity. *Scientific Reports*, *11*(1), 15133. https://doi.org/10.1038/s41598-021-92419-1

Acharya, S., Niraula, U., & Dahal, B. K. (2023). Improving soft clay behavior with alkali-activated waste eggshell for sustainable ground engineering. *International Journal of Geosynthetics and Ground Engineering*, *9*(5), 1–13. https://doi.org/10.1007/s40891-023-00480-9

Balasubramaniam, A. S., Kamruzzaman, A. H. M., Uddin, K.; Lin, D. G., Phienwij, N., & Bergado, D. T. (1998). Chemical Stabilization of Bangkok Clay with Cement, Lime and Flyash Additives. *13th SEAGC*, 253–258.

Behak, L. (2017). Soil stabilization with rice husk ash. In *Rice - Technology and Production*. InTech. https://doi.org/10.5772/66311

Broms, B. B. (1990). Stabilization of soft clay with lime and cement columns in southeast. *International Journal of Rock Mechanics and Mining Sciences & Geomechanics Abstracts*, *27*(2), A105. https://doi.org/10.1016/0148-9062(90)95192-4

Broms, B. B., & Anttikoski, U. (1984). Soil Stabilization. *Proceedings of the European Conference on Soil Mechanics and Foundation Engineering*, *3*, 1289–1315. https://doi.org/10.1201/9781482288971-15

Chai, J. C., Shen, J. S. L., Liu, M. D., & Yuan, D. J. (2018). Predicting the performance of embankments on PVD-improved subsoils. *Computers and Geotechnics*, *93*, 222–231. https://doi.org/10.1016/j.compgeo.2017.05.018

Chew, S. H., Kamruzzaman, A. H. M., & Lee, F. H. (2004). Physicochemical and Engineering Behavior of Cement Treated Clays. *Journal of Geotechnical and Geoenvironmental Engineering*, *130*(7), 696–706. https://doi.org/10.1061/(ASCE)1090-0241(2004)130:7(696)

Chhabra, R. S., & Ransinchung Rongmei Naga, G. (2023). Stabilization of cement-treated base mixes incorporating high reclaimed asphalt pavement materials using stabilizer rich in SiO2 and Al2O3. *Construction and Building Materials*, *365*, 130089. https://doi.org/10.1016/j.conbuildmat.2022.130089

Consoli, N. C., Rotta, G. V., & Prietto, P. D. M. (2006). Yielding–compressibility–strength relationship for an artificially cemented soil cured under stress. *Géotechnique*, *56*(1), 69–72. https://doi.org/10.1680/geot.2006.56.1.69

Dahal, B. K., Zheng, J.-J. J., Zhang, R.-J. J., & Song, D.-B. B. (2019). Enhancing the mechanical properties of marine clay using cement solidification. *Marine Georesources and Geotechnology*, *37*(6), 755–764. https://doi.org/10.1080/1064119X.2018.1484532

Dahal, B. K., & Zheng, J. J. (2024). Comprehensive analysis of cement-stabilised dredged marine soil: Evaluating physical, microstructural, and mechanical characteristics. *Ministry of Science and Technology, Vietnam*, *66*(2), 52–60. https://doi.org/10.31276/vjste.66(2).52-60

Dai, Z., Qin, Z., Gasparre, A., Low, H.-E., Phoon, K.-K., Kamruzzaman, A. H. M., Chew, S. H., Lee, F. H., Sridharan, A., El-Shafei, A., Miura, N., Horpibulsuk, S., Phojan, W., Suddeepong, A., Chinkulkijniwat, A., Liu, M. D., Mansouri, M., Delenne, J. Y., Seridi, A., & El Youssoufi, M. S. (2015). Dynamic Centrifuge Tests on Soft Clay Reinforced by Soil-Cement Grids. *Applied Clay Science*, *20*(IFCEE 2015), 2349–2358. https://doi.org/10.1007/s11771-013-1854-7

Dehghani, F., Kalantariasl, A., Saboori, R., Sabbaghi, S., & Peyvandi, K. (2019). Performance of carbonate calcium nanoparticles as filtration loss control agent of water-based drilling fluid. *SN Applied Sciences*, *1*(11), 1466. https://doi.org/10.1007/s42452-019-1446-8

Fil, B. A., Özmetin, C., & Korkmaz, M. (2014). Characterization and electrokinetic properties of montmorillonite. *Bulgarian Chemical Communications*, *46*(2), 258–263.

Garcia, D. C. S., Lima, K. U., Wang, K., & Figueiredo, R. B. (2022). Evaluating the effect of autoclave curing on the microstructure and compressive strength evaluation of a high strength concrete. *Matéria (Rio de Janeiro)*, *27*(2). https://doi.org/10.1590/s1517-707620220002.1301

Ghosh, A., & Subbarao, C. (2006). Leaching of Lime from Fly Ash Stabilized with Lime and Gypsum. *Journal of Materials in Civil Engineering*, *18*(1), 106–115. https://doi.org/10.1061/(ASCE)0899-1561(2006)18:1(106)

Gui, Y., Zhang, Q., Qin, X., & Wang, J. (2021). Influence of Organic Matter Content on Engineering Properties of Clays. *Advances in Civil Engineering*, *2021*(1). https://doi.org/10.1155/2021/6654121

Guo, W., Xu, S., Hong, T., Hao, S., & Chen, G. (2023). Study of Structural and Compression Properties of Soft Soils in Kunming at Different Moisture Contents. *Shock and Vibration*, *2023*, 1–10. https://doi.org/10.1155/2023/8618546

Horpibulsuk, S., Miura, N., & Nagaraj, T. S. (2003). Assessment of strength development in cement-admixed high water content clays with Abrams' law as a basis. *Géotechnique*, *53*(4), 439–444. https://doi.org/10.1680/geot.53.4.439.37319

Indraratna, B., Zhong, R., Rujikiatkamjorn, C., Choudhary, K., & Nguyen, T. T. (2016). Advances in Embankment Engineering Through Soft Ground Improvement. *Indian Geotechnical Conference, December*, 1–12.

Jan, O. Q., & Mir, B. A. (2018). Strength Behaviour of Cement Stabilised Dredged Soil. *International Journal of Geosynthetics and Ground Engineering*, *4*(2), 16. https://doi.org/10.1007/s40891-018-0133-y

Jefferson, I., Rogers, C., Evststiev, D., & Karastanev, D. (2015). Improvement of collapsible loess in Eastern Europe. In *Ground Improvement Case Histories: Compaction, Grouting and Geosynthetics* (Vol. 2). Elsevier Ltd. https://doi.org/10.1016/B978-0-08-100698-6.00007-6

K. C., N., & Raj Dahal, K. (2020). Investigation of Soil at Different Locations of the Kathmandu Valley of Nepal. *American Journal of Science, Engineering and Technology*, *5*(4), 167. https://doi.org/10.11648/j.ajset.20200504.16

K.C., S., Bhandary, N. P., & Yatabe, R. (2016). *Fundamental properties of Kathmandu clay and seismic response*. 7–8.

Kamruzzaman, A. H. M., Chew, S. H., & Lee, F. H. (2006). Microstructure of cement-treated Singapore marine clay. *Proceedings of the Institution of Civil Engineers - Ground Improvement*, *10*(3), 113–123. https://doi.org/10.1680/grim.2006.10.3.113

Kang, X., Kang, G.-C., Chang, K.-T., & Ge, L. (2015). Chemically Stabilized Soft Clays for Road-Base Construction. *Journal of Materials in Civil Engineering*, *27*(7). https://doi.org/10.1061/(ASCE)MT.1943-5533.0001156

Kang, X., Kang, G.-C., & Ge, L. (2013). Modified Time of Setting Test for Fly Ash Paste and Fly Ash–Soil Mixtures. *Journal of Materials in Civil Engineering*, *25*(2), 296–301. https://doi.org/10.1061/(ASCE)MT.1943-5533.0000604

Kang, X., Li, C., Zhang, M., Yu, X., & Chen, Y. (2024). Mechanical Properties and Stabilization Mechanism of Steel Slag-Rice Husk Ash Solidified High Plasticity Clay. *Geotechnical Testing Journal*, *47*(1). https://doi.org/10.1520/GTJ20220294

Katel, T. ., Upreti, B. ., & Pokhrel, G. . (1996). engineering properties of fine grained soils of kathmandu valley. *Journal of Nepal Geological Society*, *Vol. 13*, 121–138.

Kawasaki, T., Niina, A., Saitoh, S., Suzuki, Y., & Honjyo, Y. (1981). Deep Mixing Method Using Cement Hardening Agent. In *Technical Research Report* (Vol. 3).

Li, W., Chen, W.-S., Zhou, P.-P., & Yu, L.-J. (2013). Influence of enzyme concentration on bio-sequestration of CO2 in carbonate form using bacterial carbonic anhydrase. *Chemical Engineering Journal*, *232*, 149–156. https://doi.org/10.1016/j.cej.2013.07.069

Locat, J., Bérubé, M. A., & Choquette, M. (1990). Laboratory investigations on the lime stabilization of sensitive clays: shear strength development. *Canadian Geotechnical Journal*, *27*, 294–304.

Méducin, F., Bresson, B., Lequeux, N., Noirfontaine, M. de, & Zanni, H. (2007). Calcium silicate hydrates investigated by solid-state high resolution 1H and 29Si nuclear magnetic resonance. *Cement and Concrete Research*, *37*(5), 631–638. https://doi.org/10.1016/j.cemconres.2007.01.011

Mitchell R.J. (1970). Summary for Policymakers. In *On the yielding and mechanical strength of Leda clays* (Vol. 7, Issue 3, pp. 297–312).

Miura, N., Horpibulsuk, S., & Nagraj, T. S. (2001). Engineering behavior of cement stabilized clay at high water content. *SOILS AND FOUNDATIONS*, *41*(5), 33–45. https://doi.org/10.3208/sandf.41.5_33

Paudel, S., & Kumar, B. (2022). *Effect of Brick Dust on Soil and Strength Improvement with the use of Plastic Waste*. *8914*, 197–201.

Phuyal, P., & Dahal, B. K. (2021). *Effect of Stone Dust on Geotechnical Parameter of Fine Grained Soil*. *8914*, 1435–1440.

Porbaha, A., Shibuya, S., & Kishida, T. (2000). State of the art in deep mixing technology. Part III:geomaterial characterization. *Proceedings of the Institution of Civil Engineers - Ground Improvement*, *4*(3), 91–110. https://doi.org/10.1680/grim.2000.4.3.91

Prusinski, J. R., & Bhattacharja, S. (1999). Effectiveness of portland cement and lime in stabilizing clay soils. *Transportation Research Record*, *1*(1652), 215–227. https://doi.org/10.3141/1652-28

Qu, X., Zhao, Z., & Zhao, X. (2018). Microstructure and characterization of aluminum-incorporated calcium silicate hydrates (C–S–H) under hydrothermal conditions. *RSC Advances*, *8*(49), 28198–28208. https://doi.org/10.1039/C8RA04423F

Sachan, A., & Penumadu, D. (2007). Identification of Microfabric of Kaolinite Clay Mineral Using X-ray Diffraction Technique. *Geotechnical and Geological Engineering*, *25*(6), 603–616. https://doi.org/10.1007/s10706-007-9133-8

Saminpanya, S., & Denkitkul, N. (2020). Micromorphology, mineralogy, and geo-chemistry of sediments at the Tham Lod rock shelter archaeological site in Mae Hong Son, Thailand: suggestions of a late Pleistocene climate. *Journal of Cave and Karst Studies*, *81*(1), 51–68. https://doi.org/10.4311/2019ES0111

Sasanian, S., & Newson, T. A. A. (2014). Basic parameters governing the behaviour of cement-treated clays. *Soils and Foundations*, *54*(2), 209–224. https://doi.org/10.1016/j.sandf.2014.02.011

Shrestha, G., Shakya, B. M., Shrestha, M. B., & Khadka, U. R. (2023). Water infiltration rate in the Kathmandu Valley of Nepal amidst present urbanization and land-use change. *H2Open Journal*, *6*(1), 1–14. https://doi.org/10.2166/h2oj.2023.044

Tan, T. S., Goh, T. L., & Yong, K. Y. (2002). Properties of Singapore marine clays improved by cement mixing. *Geotechnical Testing Journal*, *25*(4), 422–433. https://doi.org/10.1520/GTJ11295J

Uddin, K., Balasubramaniam, A. S., & Bergado, D. T. (1997). Engineering behavior of cement-treated Bangkok soft clay. *Geotechnical Engineering*, *28*(1), 89–119.

Xiao, H., Wang, W., & Goh, S. H. (2017). Effectiveness study for fly ash cement improved marine clay. *Construction and Building Materials*, *157*. https://doi.org/10.1016/j.conbuildmat.2017.09.070

Zhao, H., Zhou, K., Zhao, C., Gong, B.-W., & Liu, J. (2016). A long-term investigation on microstructure of cement-stabilized handan clay. *European Journal of Environmental and Civil Engineering*, *20*(2), 199–214. https://doi.org/10.1080/19648189.2015.1030087

Zhu, X., Li, W., Zhan, L., Huang, M., Zhang, Q., & Achal, V. (2016). The large-scale process of microbial carbonate precipitation for nickel remediation from an industrial soil. *Environmental Pollution*, *219*, 149–155. https://doi.org/10.1016/j.envpol.2016.10.047